**Jurnal Elektronika dan Telekomunikasi (JET)**, Vol. 25, No. 2, December 2025, pp. 86-92
Accredited by RISTEKDIKTI, Decree No: **158/E/KPT/2021**
doi: 10.55981/jet.765

# Fabrication of Quartz Crystal Microbalance Coated with GO/PVC Nanofiber for Benzene Detection as Tuberculosis Biomarker

**Doni Bowo Nugroho*, Nada Nadzira Ayasha Kamal, Rosita Wati, Nova Resfita**

*Biomedical Engineering Study Program*
*Institut Teknologi Sumatera*
*Jl. Terusan Ryacudu, Way Huwi, Jati Agung, Lampung Selatan*
*Lampung, Indonesia 35365*

**Abstract**

Tuberculosis (TB) is a highly contagious illness and a major contributor to global mortality, with over 1.5 million deaths reported annually. TB is caused by *Mycobacterium tuberculosis* (Mtb), which is often difficult to diagnose in the early stages of infection. Existing diagnostic methods are limited by long processing times, high costs, and suboptimal sensitivity. Therefore, this study aimed to develop a Quartz Crystal Microbalance (QCM)-based biosensor employing polyvinyl chloride (PVC) nanofibers coated with graphene oxide (GO) for rapid detection of volatile TB biomarkers, particularly benzene. The sensing platform utilized a 10 MHz AT-cut silver electrode QCM coated with electrospun PVC nanofibers, followed by GO deposition via immersion. Scanning Electron Microscopy (SEM) showed uniform nanofibers with diameters increasing from 183 ± 54 nm to 348 ± 50 nm after GO coating, while FTIR confirmed the presence of GO functional groups. Sensor evaluation revealed a clear and concentration-dependent frequency shift, with a sensitivity of 1.88 Hz·L/mg, a strong linear correlation ($R^2$ = 0.99) across 1.18–23.68 mg/L, and a fast response time of 71 seconds. The limits of detection and quantification were determined to be 0.88 mg/L and 2.66 mg/L, respectively. Adsorption followed the Langmuir isotherm model, indicating monolayer uptake. These results demonstrate that the GO/PVC nanofiber-coated QCM offers a promising, low-cost, and sensitive approach for TB biomarker detection in breath analysis.

**Keywords:** benzene, graphene oxide, polyvinyl chloride, quartz crystal microbalance, tuberculosis.

## I. INTRODUCTION

Tuberculosis (TB) is a chronic infectious and contagious illness attributable to *Mycobacterium tuberculosis* (Mtb), which mainly targets the lungs but may extend to other organs [1], [2]. Due to its high transmissibility, TB remains a major global health threat, responsible for over a million deaths annually [3]–[5]. Rapid and accurate diagnosis is crucial to control its spread. It is also essential for effective disease management. However, conventional diagnostic methods still have limitations. The Interferon-γ Release Assay (IGRA) and the Mantoux tuberculin skin test (TST) take considerable time. They also show low sensitivity, especially for early-stage infections [6].

Early detection of TB can be achieved through specific biological markers. One option is to analyze volatile organic compounds (VOCs) in the breath of TB patients. These include oxidative stress products such as alkanes and their derivatives [7]. They also include volatile metabolites of Mtb, such as cyclohexane and benzene derivatives [8], [9]. Detecting such compounds provides a non-invasive approach to identifying early infection. Biosensors designed to target these biomarkers are now seen as a promising tool for rapid TB diagnosis [10]. The key challenge is to build sensors that are not only sensitive but also have a fast response time.

Quartz Crystal Microbalance (QCM) is a mass-sensitive sensor platform that shows significant potential for detecting disease biomarkers, including those of TB [4], [10]. QCM is a surface acoustic wave sensor based on the piezoelectric effect [11]. It is widely used for the measurement of tiny mass changes, even at the nanogram scale [12]. QCM detects mass changes through shifts in its resonance frequency. Sauerbrey introduced a quantitative relationship between the two values, mathematically expressed in (1) [13].

$$\Delta f = -\frac{2 f_0^2}{A\sqrt{\mu_q \rho_q}} \Delta m \quad (1)$$

In the Sauerbrey equation, $\Delta f$ denotes the frequency change of the QCM (in Hz), while $f_0$ represents its fundamental resonance frequency (in Hz). The parameters $\rho_q$ and $\mu_q$ correspond to the density (2.648 g·cm$^{-3}$) and the shear modulus ($2.947 \times 10^{11}$ g·cm$^{-1}$·s$^{-2}$) of AT-cut quartz, respectively. $\Delta m$ indicates the added mass (in grams), and $A$ refers to the electrode surface area of the quartz crystal (in cm$^2$). This equation is valid for gas-phase sensing as long as the deposited film is rigid and evenly distributed. It should also not reduce the crystal's resonant frequency by more than 2% [14].

QCM sensor performance can be improved by tailoring the active layer. This modification allows the

* Corresponding Author.
Email: doni.nugroho@bm.itera.ac.id
Received: July 6, 2025 ; Revised: September 9, 2025
Accepted: October 24, 2025 ; Published: December 31, 2025

sensor to respond more effectively to TB biomarkers. Several studies have reported the use of polymer-based QCM sensors for volatile compounds such as benzene. Active layers including polystyrene (PS), polyacrylonitrile (PAN), polyvinyl acetate (PVAc), polyvinylidene fluoride (PVDF), and polyvinylpyrrolidone (PVP) have been tested. Sensitivities ranged from 0.018 Hz/ppm to 2.50 Hz·L/mg, with response times of several hundred seconds [15]–[20]. However, these results are still too limited for rapid and sensitive detection. Therefore, active layer modification must consider the interaction between the sensing layer and TB biomarkers to improve both sensitivity and response time [21].

Modification of the QCM active layer with graphene oxide (GO) and polyvinyl chloride (PVC) nanofibers offers potential advantages in enhancing sensitivity and response time. The unique structure and excellent conductivity of GO allow for improved sensor response toward Mtb biomarkers [22], [23]. Meanwhile, PVC, a widely available and cost-effective polymer [24], can serve as a supporting nanofiber structure for GO. This nanofiber configuration provides opportunities to enhance sensitivity. Additionally, the electron-rich functional groups in PVC may interact with negatively charged groups of Mtb biomarkers, such as benzene derivatives [25]. Therefore, in this study, GO/PVC nanofibers were fabricated as the active sensing layer of a QCM sensor for benzene detection, one of the TB biomarkers. This sensor is expected to contribute to efforts in TB prevention, diagnosis, and treatment.

## II. METHODS

### A. Materials

The materials used in this work included a 10 MHz AT-cut QCM (Daishinku Corp., Indonesia), graphene oxide dispersion (PT. Inovasi Teknologi Nano, Indonesia), and polyvinyl chloride resin (Kimia Market, Indonesia). The organic solvents employed were N,N-dimethylacetamide (DMAc) (Merck, USA), and ethanol (Merck, USA), along with distilled water. The biomarker compound for *Mycobacterium tuberculosis* (Mtb), benzene, was obtained from Sigma-Aldrich (Darmstadt, Germany). All chemicals were used without modification or additional treatment.

### B. Preparation of GO/PVC Solution

Based on previous studies, PVC was completely dissolved in DMAc [26], [27]. Hence, in this work, a 7% (m/v) PVC solution was prepared by dissolving PVC in DMAc, followed by stirring for 90 minutes to ensure homogeneity for nanofiber formation. A 0.2% (m/v) GO dispersion was prepared in a 1:1 mixture of distilled water and ethanol. The GO dispersion was subsequently deposited onto the PVC nanofiber layer using an immersion technique.

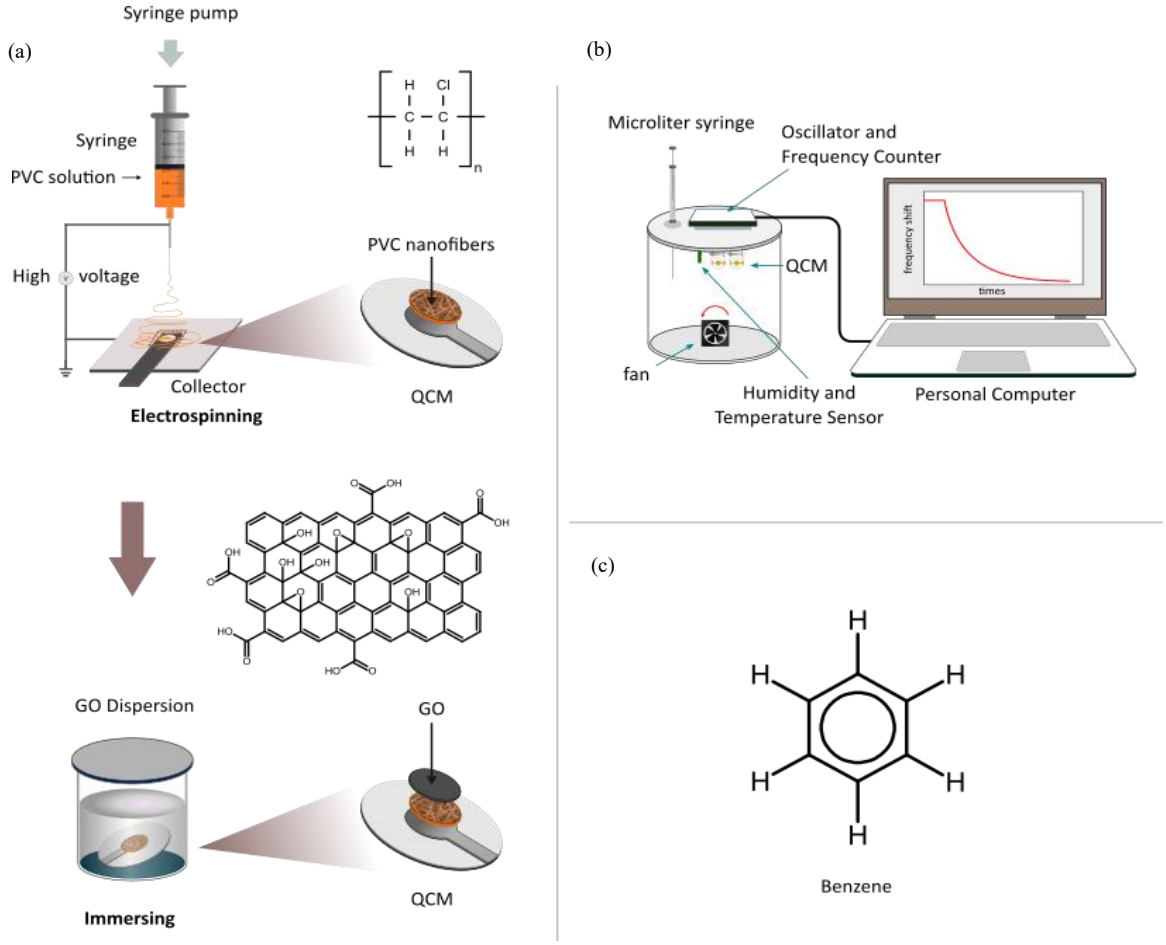


Figure 1. (a) Illustration of the coating procedure for the QCM sensor using PVC nanofibers combined with GO. (b) Setup diagram of the experimental apparatus used for vapor detection. (c) Molecular representation of benzene structure. *Sub-figures (a) and (b) are modified from* [28]*, used under CC BY 4.0.*

### C. Deposition of GO/PVC Layer onto QCM

This work employed a combination of electrospinning and immersion methods, similar to those used in previous studies [28]. The PVC solution was deposited onto the surface of the QCM using an electrospinning instrument (ILMI-N101, Indonesia). The solution was placed in a 10 mL syringe and delivered through a needle connected to a 12.5 kV high-voltage power supply. The needle-to-collector gap was 15 cm, with a solution flow rate of 0.005 mL/min. The QCM coated with PVC nanofibers was then immersed in the GO dispersion for 10 seconds and subsequently dried at room temperature. This process is illustrated in Figure 1a.

### D. Characterization of the GO/PVC Layer

Morphological and chemical analysis was conducted to evaluate the surface structure of the PVC nanofibers before and after the deposition of GO. The fiber morphology was examined using scanning electron microscopy (SEM, Zeiss EVO 10) at 20 kV [29]. This examination included the shape of the fibers and their diameter distribution. The average fiber diameter and its distribution were determined from the SEM images using image analysis software (ImageJ). In addition, the chemical composition was analyzed using Fourier-transform infrared spectroscopy (FTIR). The method was further utilized to investigate the functional groups of GO on the PVC nanofiber surface.

### E. Characterization of Sensor Response

The response of the sensor to the analyte was measured using a custom-designed sensor chamber, based on previous studies [28], [30], as illustrated in Figure 1b. The chamber, with a total volume of 3.7 liters, was constructed from stainless steel. A low-voltage DC fan (12 V) was installed at the base of the chamber to ensure homogeneous distribution of the analyte. The top cover of the chamber was equipped with an oscillator circuit for the QCM channel, integrated with a frequency counter and additional circuits for temperature, humidity, and pressure sensing. The concentration was expressed in mg/L [30].

## III. Results and Discussion

### A. QCM Sensor with GO/PVC Coating

Figure 2a displays the uncoated QCM sensor. It consists of a 10 MHz AT-cut quartz crystal (HC-49U package) with its protective casing removed to expose the active sensing surface. The circular silver electrodes, each approximately 3.74 mm in diameter, were deposited symmetrically on both sides of the quartz substrate. In this pristine state, the electrodes exhibited a smooth and reflective surface without any material deposition. This configuration served as the reference state for mass loading measurements.

Figure 2b shows the same QCM sensor after functionalization with PVC nanofibers via electrospinning and a thin layer of GO applied via immersion. The deposition was successful and homogeneous. The composite film formed a uniform and continuous layer across the electrode surface, as observed visually.

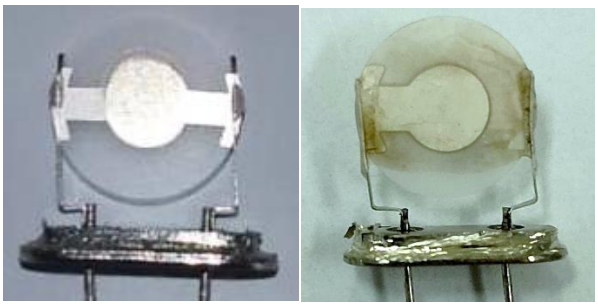

(a) (b)

Figure 2. (a) QCM without material deposition and (b) QCM with GO/PVC nanofiber layer.

The QCM resonant frequency was measured before and after material deposition. The frequency decreased by 3603 Hz after PVC deposition and by 4714 Hz following GO immersion. According to the Sauerbrey equation, these decreases correspond to mass increases of approximately 1748 ng and 2287 ng, respectively. These frequency changes indicate the successful deposition of the active layer on the sensor.

### B. Characteristics of GO/PVC Layer

Figure 3a shows the SEM image of the electrospun PVC nanofiber layer. The fibers form a dense and uniform network. They are evenly distributed across the substrate. This indicates that the electrospinning process was consistent and produced a homogeneous fibrous mat. Such morphology is beneficial for sensor applications. The large surface area and porous structure help improve analyte interaction and adsorption efficiency [31].

Figure 3b presents the SEM image of the PVC nanofiber layer after being coated with graphene oxide (GO) via immersion. The surface appears smoother and less textured compared to Figure 3a. Fiber-like features are still faintly visible beneath the top layer. This suggests that the GO film partially or fully covered the nanofiber matrix. The smooth appearance is consistent with the planar nature of GO, which tends to spread evenly during immersion. This composite structure demonstrates successful deposition of GO. The GO layer can enhance the sensor's chemical sensitivity by providing additional active sites and improving surface conductivity [23], [32].

Figure 3c-d shows the fiber diameter distribution of the nanofiber layers before and after the deposition of graphene oxide (GO). The electrospun PVC nanofibers had an average diameter of 183 ± 54 nm. After coating with GO via immersion, the average diameter increased significantly to 348 ± 50 nm. This added thickness suggests that the GO layer successfully covered the nanofibers.

FTIR spectroscopy analysis was performed to verify the existence of graphene oxide on the PVC nanofiber surface. Figure 4 depicts the FTIR spectra obtained for PVC nanofibers and GO/PVC nanofibers. The PVC nanofibers spectrum in Figure 4a shows an absorption band at 657 $cm^{-1}$. This band corresponds to the C–Cl stretching vibration. It confirms the PVC backbone [33]. Other PVC-related features include C–H

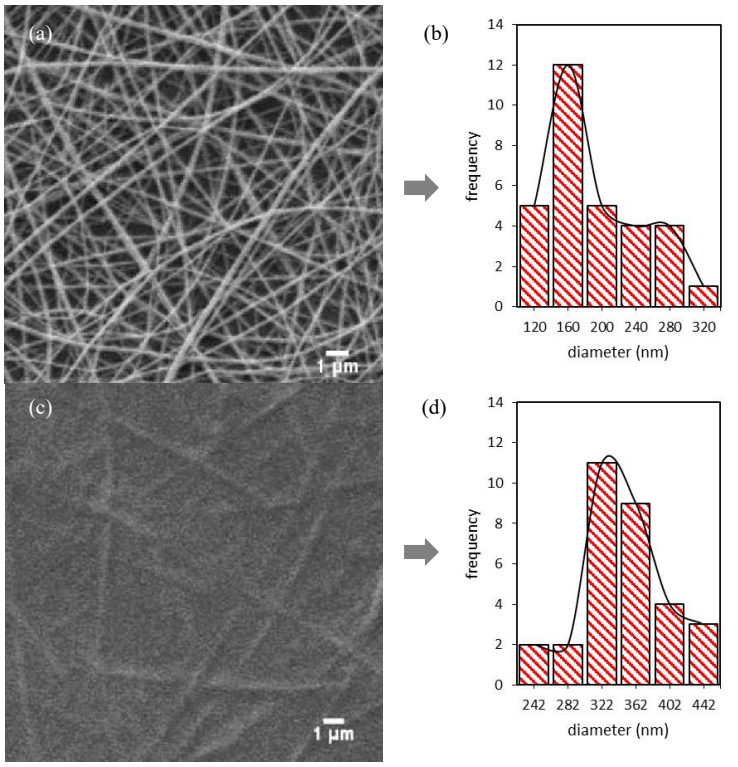


Figure 3. SEM images of (a) PVC nanofibers and (b) GO/PVC nanofibers. Diameter distribution of (c) PVC nanofibers and (d) GO-coated PVC nanofibers.

stretching vibrations at 2908 $cm^{-1}$. $CH_2$ bending vibrations appear at 1425 $cm^{-1}$. These features are consistent with previously reported spectra of neat PVC [33]–[35].

The FTIR spectrum of GO/PVC nanofibers (Figure 4b) shows bands almost characteristic of both GO and PVC nanofibers. The spectrum shows an additional band at 1065 $cm^{-1}$, which is assigned to C–O stretching of alkoxy groups [36]. Another band is observed at 1220 $cm^{-1}$, characteristic of C–O–C stretching vibrations from epoxy functionalities [34]. Furthermore, a wide absorption band between 3200 and 3600 $cm^{-1}$ indicates the existence of hydroxyl groups (O–H stretching) [34]. The expected C=O stretching vibration at ~1715-1730 $cm^{-1}$, usually associated with carboxyl groups in graphene oxide, was only slightly prominent in this sample [36]. This may be due to the relatively low content of GO in the composite, which reduces the abundance of carbonyl functionalities. The presence of both PVC and GO-related bands confirms the incorporation of graphene oxide into the PVC nanofibers.

## C. Frequency Response of QCM Sensor to Benzene Vapor

Three variants of QCM sensors were prepared to evaluate the effect of coating materials on frequency response: QCM blank (QCM 0), QCM coated with GO layer (QCM GO), and QCM coated with GO/PVC nanofibers (QCM GO/PVC nanofibers). The sensor responses were evaluated under exposure to a fixed concentration of benzene vapor (11.84 mg/L). It can be seen in Figure 5 that QCM 0 exhibited almost no frequency shift when exposed to benzene vapor, indicating negligible sensitivity. In contrast, the QCM GO sensor showed a clear response with a negative

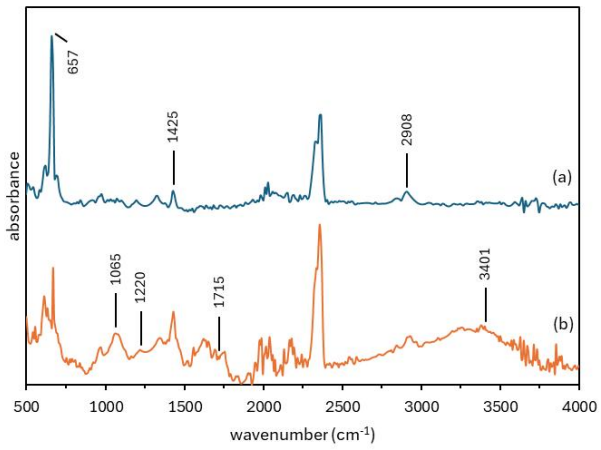


Figure 4. FTIR spectrum of (a) PVC resin and (b) GO/PVC nanofibers.

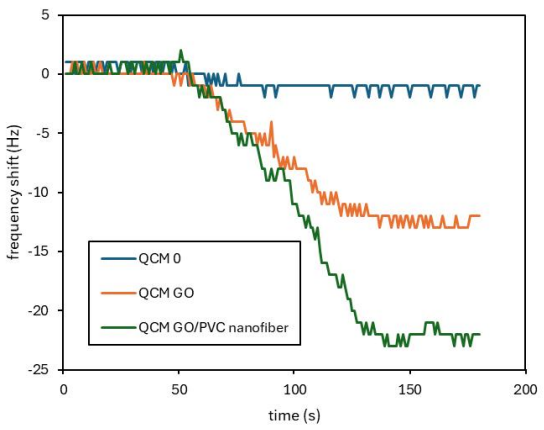


Figure 5. Characteristic response of the different coating materials of QCM sensors at 11.84 mg/L benzene.

frequency shift of about 10 Hz. This response is likely associated with the adsorption of benzene molecules on the oxygen-containing groups of GO.

The QCM GO/PVC nanofiber sensor exhibited a much stronger response, reaching a frequency shift of approximately 23 Hz. This frequency shift may be attributed to the synergistic effect of GO and PVC nanofibers. The combination provides a larger surface area and additional adsorption sites for benzene molecules. The nanofiber network offers a high surface area and porosity, while the GO provides abundant oxygen-containing functional groups that facilitate π–π interactions with aromatic benzene molecules [37]–[39]. This results in increased mass uptake on the crystal surface, reflected by the frequency shift.

The QCM GO/PVC nanofiber sensor was tested with benzene vapor at different concentrations within the concentration range of 1.18–23.68 mg/L (see Figure 6a). The frequency shift increased as the benzene concentration increased. At concentrations of 1.18, 2.37, 4.74, 11.84, and 23.68 mg/L, the frequency shifts reached approximately 3.3, 5.7, 10.3, 22.3, and 44.0 Hz, respectively. Measurements were repeated three times (n = 3) for repeatability. Afterward, the chamber was purged with ambient air to allow recovery of the frequency baseline.

The linear correlation between benzene concentration and frequency shift is presented in Figure 6b. A linear fitting yielded a sensitivity ($S$) of 1.88 Hz·L/mg with excellent linearity, as shown by the determination coefficient ($R^2$) of 0.99 in the concentration range of 1.18–23.68 mg/L. The standard deviation ($\sigma$) of the blank signal was measured as 0.5 Hz. This value was then used to determine the limit of detection (LOD) using the formula LOD = $3.3\sigma/S$. Subsequently, it was also used to determine the limit of quantification (LOQ) using the formula LOQ = $10\sigma$/S. Based on these calculations, the QCM GO/PVC nanofiber sensor exhibited an LOD of about 0.88 mg/L and an LOQ of approximately 2.66 mg/L for benzene vapor detection. These values indicate that the sensor has high sensitivity and reliable detection capability for benzene vapor.

The Langmuir isotherm model is commonly applied to describe the adsorption kinetics behaviour in QCM. The approach was utilized to analyze the sorption dynamic of benzene molecules onto the GO/PVC nanofiber surface [40]. The variation of benzene uptake on the GO/PVC nanofiber surface over time ($\Delta m_t$) is described by (2):

$$\Delta m_t = \Delta m_\infty \left(1 - e^{-t/\tau}\right) \quad (2)$$

where $\Delta m_\infty$ represents the maximum adsorption capacity of benzene molecules on the surface as time approaches infinity ($t \rightarrow \infty$), and $t$ refers to the relaxation time. The parameter of $\Delta m_t$ can be calculated according to the Sauerbrey equation ( $\Delta m = (4.85\text{ng/Hz})\Delta f$ ) [28], [41].

Figure 7 illustrates the Langmuir model fitting (Equation (2)) to experimental data for 4.74 mg/L benzene, with the red solid line indicating the fitted curve. The maximum adsorbed mass ($\Delta m_\infty$) was determined to be 5.45 ng, with a response time ($\tau$) of 31 seconds. These findings indicate that the adsorption of benzene on the GO/PVC nanofiber surface follows the Langmuir isotherm behavior closely ($R^2 = 0.95$).

Table 1 provides a comparison between the GO/PVC nanofiber-coated QCM sensor developed in this work and previously reported polymer-coated QCM sensors for benzene detection. The table lists the QCM type, polymer material, deposition method, sensitivity, and response time. Reported polymer-coated QCMs with gold electrodes (e.g., PS, PAN, PVAc, PVDF, PVP) generally show sensitivities in the range of 0.018 Hz/ppm to 2.5 Hz·L/mg [15]–[20], but often exhibit

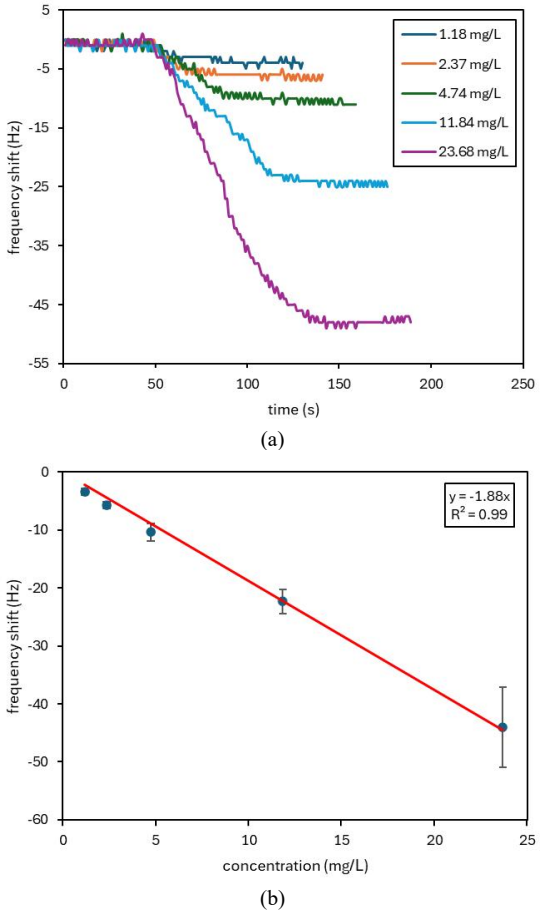


Figure 6. (a) Response of the QCM GO/PVC nanofiber sensor at different benzene concentrations. (b) Calibration plot illustrating the sensitivity of the sensor to benzene vapor.

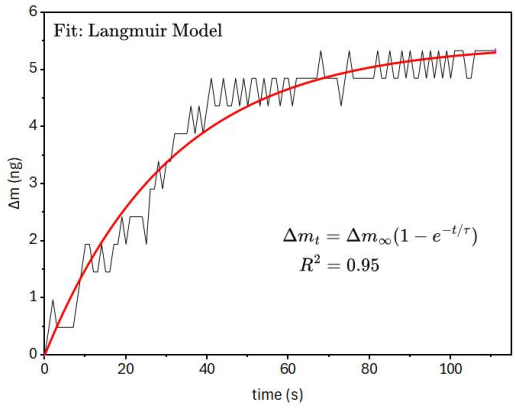


Figure 7. Langmuir isotherm fitting of the QCM GO/PVC nanofiber sensor in response to 4.74 mg/L benzene.

TABLE 1
COMPARATIVE EVALUATION OF THE GO/PVC NANOFIBER-COATED QCM SENSOR FOR BENZENE DETECTION IN REFERENCE TO PREVIOUSLY REPORTED POLYMER-FUNCTIONALIZED QCM SENSORS.

| QCM Type | Materials | Deposition Method | Sensitivity | | Response Time (s) | Year | Ref. |
|---|---|---|---|---|---|---|---|
| | | | (Hz/ppm) | (Hz·L/ mg) | | | |
| 10 MHz Gold Electrode | Polystyrene | Casting | 1.33 | – | 260 | 2006 | [15] |
| 10 MHz Gold Electrode | PAN | Electrospinning | – | ~0.50 | – | 2018 | [16] |
| 10 MHz Gold Electrode | PVAc | Electrospinning | 0.018 | – | 225 | 2019 | [17] |
| 10 MHz Gold Electrode | PAN | Spin coating | – | 0.40 | – | 2020 | [18] |
| 10 MHz Gold Electrode | PVDF/PVAc | Spin coating | – | ~1.00 | – | 2020 | [18] |
| 10 MHz Gold Electrode | PVP | Spin coating | – | ~2.00 | – | 2020 | [18] |
| 10 MHz Gold Electrode | PVAc | Spin coating | – | ~2.50 | – | 2020 | [18] |
| 5 MHz | PEMA–DIOA (5 %) | Spin coating | – | – | 220 | 2021 | [19] |
| – | PVAc | Spin coating | 0.109 | – | – | 2023 | [20] |
| 10 MHz Silver Electrode | GO/PVC | Electrospinning-Immersing | – | 1.88 | 71 | 2025 | This work |

"–" indicates that the data is not explicitly reported in the literature.

"~" indicates that the value is approximated from a figure or graph in the literature.

long response times–sometimes extending to several hundred seconds–which limits their applicability for rapid detection.

In contrast, the QCM GO/PVC nanofiber developed in this study showed improved sensing performance. It achieved a sensitivity of 1.88 Hz·L/mg. The response time was 71 seconds. The performance improvement is likely due to the nanofiber morphology and the GO/PVC composite. These features provide more adsorption sites and enhance diffusion. Compared with most previously reported polymer-coated QCMs, the sensor shows a faster response. This indicates a practical advantage for benzene detection.

## IV. CONCLUSION

This research successfully fabricated and evaluated a GO/PVC nanofiber-functionalized QCM sensor for the sensing of benzene vapor as a model biomarker of *Mycobacterium tuberculosis* (Mtb). The incorporation of GO into PVC nanofibers was confirmed by SEM and FTIR, and sensor evaluation revealed a high sensitivity of 1.88 Hz·L/mg, a low detection limit of 0.88 mg/L, and a rapid response time of 71 seconds. Compared with previously reported polymer-based QCM sensors, the GO/PVC nanofiber-coated QCM exhibited enhanced performance due to the synergy between nanofiber morphology and GO functionalities. These results highlight the promise of this sensor in enabling rapid and sensitive detection of benzene in breath samples for early TB diagnosis.

## DECLARATIONS

### Conflict of Interest

The authors have declared that no competing interests exist.

### CRediT Authorship Contribution

Doni Bowo Nugroho: Conceptualization, Formal analysis, Writing-Original Draft, Writing-Reviewing and Editing, Validation, Visualization, Supervision; Nada Nadzira Ayasha Kamal: Investigation, Data Curation; Rosita Wati: Writing-Reviewing and Editing, Project Administration; Nova Resfita: Writing-Reviewing and Editing, Supervision.

### Funding

This research was fully supported by Direktorat Jenderal Pendidikan Tinggi, Riset, Teknologi dan Pengabdian kepada Masyarakat–Kementerian Pendidikan Tinggi, Sains, dan Teknologi under the 2024 Research Funding Program scheme "Penelitian Dosen Pemula" through main grant number 039/E5/PG.02.00.PL/2024 and derivative contract number 1570aa/IT9.2.1/PT.01.03/2024.

### Acknowledgment

The authors would like to thank the Direktorat Jenderal Pendidikan Tinggi, Riset, Teknologi, dan Pengabdian kepada Masyarakat–Kementerian Pendidikan Tinggi, Sains, dan Teknologi, which has provided the foundation.

## REFERENCES

[1] D. Goletti, G. Meintjes, B. B. Andrade, A. Zumla, and S. Shan Lee, "Insights from the 2024 who global tuberculosis report – more comprehensive action, innovation, and investments required for achieving WHO end TB goals," *Int. J. Infect. Dis.*, vol. 150, 2025, Art. no. 107325, doi: 10.1016/j.ijid.2024.107325.

[2] J. Huang, Q. He, L. Huang, L. Liu, P. Yang, and M. Chen, "Discovering the link between IL12RB1 gene polymorphisms and tuberculosis susceptibility: A comprehensive meta-analysis," *Front. Public Heal.*, vol. 12, Jan. 2024, Art. no. 1249880, doi: 10.3389/fpubh.2024.1249880.

[3] J. Yang, L. Zhang, W. Qiao, and Y. Luo, "*Mycobacterium tuberculosis*: Pathogenesis and therapeutic targets," *MedComm*, vol. 4, no. 5, 2023, Art. no. e353, doi: 10.1002/mco2.353.

[4] H. Joshi, D. Kandari, S. S. Maitra, and R. Bhatnagar, "Biosensors for the detection of *Mycobacterium tuberculosis*: A comprehensive overview," *Crit. Rev. Microbiol.*, vol. 48, no. 6, pp. 784–812, 2022, doi: 10.1080/1040841X.2022.2035314.

[5] F. Estaji, A. Kamali, and M. Keikha, "Strengthening the global response to tuberculosis: Insights from the 2024 who global TB report," *J. Clin. Tuberc. Other Mycobact. Dis.*, vol. 39, 2025, Art. no. 100522, doi: 10.1016/j.jctube.2025.100522.

[6] N. Mohammadnabi *et al.*, "*Mycobacterium tuberculosis*: The mechanism of pathogenicity, immune responses, and diagnostic challenges.," *J. Clin. Lab. Anal.*, vol. 38, Dec. 2024, Art. no. e25122, doi: 10.1002/jcla.25122.

[7] M. Phillips *et al.*, "Volatile biomarkers of pulmonary tuberculosis in the breath," *Tuberculosis*, vol. 87, no. 1, pp. 44–52, 2007, doi: 10.1016/j.tube.2006.03.004.

[8] A. M. I. Saktiawati, D. D. Putera, A. Setyawan, Y. Mahendradhata, and T. S. van der Werf, "Diagnosis of tuberculosis through breath test: A systematic review," *EBioMedicine*, vol. 46, pp. 202–214, 2019, doi: 10.1016/j.ebiom.2019.07.056.

[9] M. Phillips *et al.*, "Breath biomarkers of active pulmonary tuberculosis," *Tuberculosis*, vol. 90, no. 2, pp. 145–151, 2010,

doi: 10.1016/j.tube.2010.01.003.
[10] S. K. Srivastava, C. J. M. Van Rijn, and M. A. Jongsma, "Biosensor-based detection of tuberculosis," *RSC Adv.*, vol. 6, no. 22, pp. 17759–17771, 2016, doi: 10.1039/c5ra15269k.
[11] Y. Zhao, Z. Li, Y. Xia, Q. Jia, L. Zhao, and R. Maboudia, "Advances in micro- and nano-scale resonant mass-sensitive gas sensors: mechanisms, materials, functionalization and applications," *Sensors Actuators B. Chem.*, vol. 431, Feb. 2025, Art. no. 137415, doi: 10.1016/j.snb.2025.137415.
[12] W. Huang *et al.*, "Highly sensitive formaldehyde sensors based on polyvinylamine modified polyacrylonitrile nanofibers," *RSC Adv.*, vol. 3, no. 45, 2013, Art. no. 22994, doi: 10.1039/c3ra44671a.
[13] G. Sauerbrey, "Verwendung von schwingquarzen zur wagungdiinner schichten und zur mikrowagung," (in German), *Zeitschrift fur. Phys.*, vol. 155, no. 2, pp. 206–222, 1959, doi: 10.1007/BF01337937.
[14] D. Johannsmann, *The Quartz Crystal Microbalance in Soft Matter Research*. Switzerland: Springer International Publishing, 2015. doi: 10.1007/978-3-319-07836-6.
[15] A. Mirmohseni and K. Rostamizadeh, "Quartz crystal nanobalance in conjunction with principal component analysis for identification of volatile organic compounds," *Sensors*, vol. 6, pp. 324–334, 2006, doi: 10.3390/s6040324.
[16] A. Rianjanu *et al.*, "Polyacrylonitrile nanofiber-based quartz crystal microbalance for sensitive detection of safrole," *Sensors (Switzerland)*, vol. 18, no. 4, 2018, Art. no. 1150, doi: 10.3390/s18041150.
[17] A. Rianjanu, S. A. Hasanah, D. B. Nugroho, A. Kusumaatmaja, R. Roto, and K. Triyana, "Polyvinyl acetate film-based quartz crystal microbalance for the detection of benzene, toluene, and xylene vapors in air," *Chemosensors*, vol. 7, no. 2, 2019, Art. no. 20, doi: 10.3390/chemosensors7020020.
[18] T. Julian, S. N. Hidayat, A. Rianjanu, A. B. Dharmawan, H. S. Wasisto, and K. Triyana, "Intelligent mobile electronic nose system comprising a hybrid polymer-functionalized quartz crystal microbalance sensor array," *ACS Omega*, vol. 5, no. 45, pp. 29492–29503, 2020, doi: 10.1021/acsomega.0c04433.
[19] A. Iyer, V. Mitevska, J. Samuelson, S. Campbell, and V. R. Bhethanabotla, "Polymer–plasticizer coatings for BTEX detection using quartz crystal microbalance," *Sensors*, vol. 21, 2021, Art. no. 5667, doi: 10.3390/s21165667.
[20] A. Das and R. Manjunatha, "Optimization of qcm sensor for btx detection," in *Proc. 2023 IEEE 9th Int. Conf. Smart Instrumentation, Meas. Appl.*, 2023, pp. 225–229. doi: 10.1109/ICSIMA59853.2023.10373452.
[21] N. Alanazi, M. Almutairi, and A. N. Alodhayb, "A review of quartz crystal microbalance for chemical and biological sensing applications," *Sens. Imaging,* vol. 24, no. 1, 2023, Art. no. 10, doi: 10.1007/s11220-023-00413-w.
[22] A. Javed, S. R. Abbas, M. U. Hashmi, N. U. A. Babar, and I. Hussain, "Graphene oxide based electrochemical genosensor for label free detection of *Mycobacterium tuberculosis* from raw clinical samples," *Int. J. Nanomedicine*, vol. 16, pp. 7339–7352, 2021, doi: 10.2147/IJN.S326480.
[23] E. N. Azizah *et al.*, "Comparative analysis of charge recombination dynamics in dye-sensitized solar cells with different counter electrodes," *J. Elektron. dan Telekomun.*, vol. 25, no. 1, pp. 1–8, Aug. 2025, doi: 10.55981/jet.703.
[24] L. Q. Pham, M. V. Uspenskaya, R. O. Olekhnovich, and R. A. O. Bernal, "A review on electrospun PVC nanofibers: Fabrication, properties, and application," *Fibers*, vol. 9, no. 2, 2021, Art. no. 12, doi: 10.3390/fib9020012.
[25] N. S. Chong, S. Abdulramoni, D. Patterson, and H. Brown, "Releases of fire-derived contaminants from polymer pipes made of polyvinyl chloride," vol. 7, 2019, Art. no. 57, doi: 10.3390/toxics7040057.
[26] A. Zulfi, S. Hartati, S. Nur'aini, A. Noviyanto, and M. Nasir, "Electrospun nanofibers from waste polyvinyl chloride loaded silver and titanium dioxide for water treatment applications," *ACS Omega*, vol. 8, no. 26, pp. 23622c23632, 2023, doi: 10.1021/acsomega.3c01632.
[27] G. Grause, S. Hirahashi, H. Toyoda, T. Kameda, and T. Yoshioka, "Solubility parameters for determining optimal solvents for separating PVC from PVC-coated PET fibers," *J. Mater. Cycles Waste Manag.*, vol. 19, no. 2, pp. 612–622, 2017, doi: 10.1007/s10163-015-0457-9.
[28] D. B. Nugroho, A. Rianjanu, K. Triyana, A. Kusumaatmaja, and R. Roto, "Quartz crystal microbalance-coated cellulose acetate nanofibers overlaid with chitosan for detection of acetic anhydride vapor," *Results Phys.*, vol. 15, 2019, Art. no. 102680, doi: 10.1016/j.rinp.2019.102680.
[29] A. D. Oktaviani and R. V. Manurung, "Screen-printed carbon electrode modified GNPs/ZnO for electrochemical biosensing," *J. Elektron. dan Telekomun.*, vol. 24, no. 1, pp. 38–45, 2024, doi: 10.55981/jet.593.
[30] A. Rianjanu, K. Triyana, D. B. Nugroho, A. Kusumaatmaja, and R. Roto, "Electrospun polyvinyl acetate nanofiber modified quartz crystal microbalance for detection of primary alcohol vapor," *Sensors Actuators, A Phys.*, vol. 301, 2020, Art. no. 111742, doi: 10.1016/j.sna.2019.111742.
[31] S. M. Nokandeh *et al.*, "Nanoporous structures-based biosensors for environmental and biomedical diagnostics: Advancements, opportunities, and challenges," *Coord. Chem. Rev.*, vol. 522, 2025, Art. no. 216245, doi: 10.1016/j.ccr.2024.216245.
[32] H. Moustafa, M. Morsy, M. A. Ateia, and F. M. Abdel-Haleem, "Ultrafast response humidity sensors based on polyvinyl chloride/graphene oxide nanocomposites for intelligent food packaging," *Sensors Actuators, A Phys.*, vol. 331, 2021, Art. no. 112918, doi: 10.1016/j.sna.2021.112918.
[33] Faiza, A. Khattak, A. A. Alahmadi, H. Ishida, and N. Ullah, "Improved PVC/ZnO nanocomposite insulation for high voltage and high temperature applications," *Sci. Rep.*, vol. 13, 2023, Art. no. 7235, doi: 10.1038/s41598-023-31473-3.
[34] K. Deshmukh, S. M. Khatake, and G. M. Joshi, "Surface properties of graphene oxide reinforced polyvinyl chloride nanocomposites," *J. Polym. Res.*, vol. 20, no. 11, 2013, Art. no. 286, doi: 10.1007/s10965-013-0286-2.
[35] B. Çobanoglu, F. N. Parin, and K. Yildirim, "Production and characterization of n-halamine based polyvinyl chloride (PVC) nanowebs," *Tekst. ve Konfeksiyon*, vol. 31, no. 3, pp. 147–155, 2021, doi: 10.32710/tekstilvekonfeksiyon.717601.
[36] V. Brusko, A. Khannanov, A. Rakhmatullin, and A. M. Dimiev, "Unraveling the infrared spectrum of graphene oxide," *Carbon*, vol. 229, 2024, Art. no. 119507, doi: 10.1016/j.carbon.2024.119507.
[37] A. Khan *et al.*, "The effect of diverse metal oxides in graphene composites on the adsorption isotherm of gaseous benzene," *Environ. Res.*, vol. 172, pp. 367–374, 2019, doi: 10.1016/j.envres.2019.01.050.
[38] L. Yu *et al.*, "Adsorption of VOCs on reduced graphene oxide," *J. Environ. Sci. (China)*, vol. 67, pp. 171–178, 2018, doi: 10.1016/j.jes.2017.08.022.
[39] P.-P. Zhou and R.-Q. Zhang, "Physisorption of benzene derivatives on graphene: Critical roles of steric and stereoelectronic effects of the substituent.," *Phys. Chem. Chem. Phys.*, vol. 17, no. 18, pp. 12185–12193, May 2015, doi: 10.1039/c4cp05973e.
[40] A. Das, R. Manjunatha, K. N. Kumar, D. De, and R. Bandyopadhyay, "Fabrication of surface functionalized QCM sensor for BTX detection at ambient conditions," *Talanta*, vol. 283, 2025, Art. no. 127081, doi: 10.1016/j.talanta.2024.127081.
[41] A. Bayram, C. Özbek, M. Şenel, and S. Okur, "CO gas sorption properties of ferrocene branched chitosan derivatives," *Sensors Actuators B Chem.*, vol. 241, pp. 308–313, 2017, doi: https://doi.org/10.1016/j.snb.2016.08.175.